

# tRNA modification and codon usage control pathogen secretion in host cells

**Gang Li**

University of Nebraska-Lincoln

**Ziwen Gong**

University of Nebraska-Lincoln

**Nawaraj Dulal**

University of Nebraska-Lincoln

**Richard Wilson** (✉ [rwilson10@unl.edu](mailto:rwilson10@unl.edu))

University of Nebraska-Lincoln <https://orcid.org/0000-0002-7754-7712>

---

## Article

### Keywords:

**Posted Date:** June 8th, 2022

**DOI:** <https://doi.org/10.21203/rs.3.rs-1690424/v1>

**License:** © ⓘ This work is licensed under a Creative Commons Attribution 4.0 International License.

[Read Full License](#)

---

**Version of Record:** A version of this preprint was published at Nature Microbiology on August 10th, 2023.

See the published version at <https://doi.org/10.1038/s41564-023-01443-6>.

# Abstract

Animal and plant microbial pathogens deploy effector proteins and virulence factors to manipulate host cell innate immunity, often using unconventional secretion routes that are poorly understood. Transfer RNA (tRNA) anticodon modifications occur across taxa, but few biological functions are known. Here, in the devastating blast fungus *Magnaporthe oryzae*, we find that unconventional protein secretion in living host rice cells depends on tRNA modification and codon usage. Using gene deletions, mass spectrometry and live-cell imaging, we characterized the *M. oryzae* Uba4-Urm1 sulfur relay system mediating tRNA anticodon wobble uridine 2-thiolation ( $s^2U_{34}$ ), a conserved modification required for efficient decoding of AA-ending cognate codons. In *M. oryzae*, cytoplasmic effectors like Pwl2 and AVR-Pita are translocated into host cells via an unconventional secretion route; apoplastic effectors like Bas4 are secreted by the conventional ER-Golgi pathway. Loss of  $U_{34}$  thiolation abolished *PWL2* and *AVR-PITA* (but not *BAS4*) mRNA translation in host cells. Paromomycin treatment, which increases near-cognate tRNA acceptance, restored Pwl2 and AVR-Pita production in  $U_{34}$  thiolation-deficient mutant strains. Synonymous AA- to AG-ending codon changes remediated *PWL2* mRNA translation in  $\Delta uba4$ ; in *UBA4<sup>t</sup>*, expressing recoded *PWL2* resulted in Pwl2 super-secretion that destabilized the microbe-host cell interface. Thus, wobble  $U_{34}$  tRNA thiolation and codon usage tune pathogen unconventional protein secretion in host cells.

## Introduction

tRNA nucleoside modifications are abundant and occur across all domains of life<sup>1-5</sup>, but biological relevance for many is poorly understood<sup>3,4,6-9</sup>. The genome of the devastating rice blast fungus *Magnaporthe oryzae*<sup>10-14</sup> carries a *UBA4* orthologue (MGG\_05569) encoding the evolutionary conserved E1-like Urm1-activating enzyme, and MGG\_03978, encoding the Uba4 substrate Ubiquitin Related Modifier 1 (Urm1). In eukaryotes, Uba4 and Urm1 act together to modify tRNA anticodon bases with sulfur<sup>15</sup>. By retaining these genes, we hypothesized that *M. oryzae* tRNA anticodon thiolation may be required for host rice plant infection.

The Uba4-Urm1 sulfur relay system is required for 2-thiolation of position 34 wobble uridines ( $s^2U_{34}$ ) in the anticodon loop of cytoplasmic (but not mitochondrial) tRNAs<sup>6,15,16</sup> (Fig. 1a).  $s^2U_{34}$  is an almost universal modification on tRNAs decoding AA-ending codons (Fig. 1a)<sup>1-3,7,17</sup>. A methoxycarbonylmethyl group ( $mcm^5$ ) also decorates  $U_{34}$ , and the loss of both modifications is lethal<sup>1</sup>.  $U_{34}$  thiolation involves the transfer of sulfur from the ubiquitin-like Urm1 following its activation by Uba4<sup>7,15,16,18</sup> (Fig. 1a). The loss of  $U_{34}$  thiolation (but not  $mcm^5$ <sup>(7)</sup>) slows cognate codon decoding, causing ribosome pausing and resulting in reduced translation speeds and increased protein aggregation<sup>3,6-8,17</sup>. Despite its ubiquity, however, a yeast  $\Delta uba4$  mutant is viable<sup>4</sup> and, although  $U_{34}$  thiolation connects translation rates to sulfur availability<sup>6</sup>, maintains metabolic homeostasis independent of translation<sup>9</sup> and also ensures efficient

stress gene translation<sup>6,7,16,19</sup>, overall, translation defects in s<sup>2</sup>U<sub>34</sub> mutants are minor<sup>3,9</sup> and few physiological roles for the anticodon wobble U<sub>34</sub> thiolation modification are known<sup>4,6,7,9,17</sup>.

To test our hypothesis that 2-thiolation of wobble uridines in *M. oryzae* tRNA anticodons are required for host plant infection, we functionally characterized the *M. oryzae* Uba4-Urm1 sulfur relay system. In doing so, we discovered an unexpected connection between U<sub>34</sub> thiolation-dependent efficient decoding of AA-ending cognate codons during mRNA translation and the unconventional secretion of cytoplasmic effector proteins targeting the host cell. Animal and plant pathogens, including *M. oryzae*, deploy immune modulating effector proteins and virulence factors to subvert the host cell for infection<sup>20</sup>, most of which are secreted by the canonical ER-Golgi network but a subset of which are secreted by complex alternative routes<sup>21–24</sup> whose underpinning mechanisms are only starting to emerge<sup>24</sup>. Here we show that tRNA U<sub>34</sub> thiolation is not required for the translation of mRNAs encoding an ER-Golgi secreted apoplastic effector (even though they carry AA-ending codons) but is required for the translation of mRNAs encoding unconventionally secreted cytoplasmic effector proteins. Synonymous AA-ending to AG-ending codon recoding in cytoplasmic effector mRNA resulted in protein super-secretion. When all our results are considered together, we conclude that the U<sub>34</sub> thiolation-dependent efficient decoding of AA-ending cognate codons in cytoplasmic effector mRNAs controls mRNA translation speeds to optimize nascent peptide synthesis under the specific folding constraints of the unconventional protein secretion pathway. By uncovering a fundamental link between codon usage, codon decoding efficiency and unconventional protein secretion, our work has wide-ranging implications for improving our basic understanding of how microbes cause disease in addition to furnishing a previously unknown and biologically relevant role for the universal tRNA anticodon thiolation modification.

## Results

### The *M. oryzae* *UBA4* and *URM1* genes are required for rice infection

To determine whether *M. oryzae* tRNA thiolation is required for rice infection, we first disrupted *UBA4* in the genome of our wild type (WT) isolate Guy11 by homologous recombination using *ILV1* as a selectable marker conferring sulphonyl urea resistance<sup>25</sup>. Three independent *Duba4*-carrying mutant strains were recovered, and each had identical phenotypes (**Extended Data Fig. 1a-e**). One deletant was used to generate the *Duba4 UBA4-GFP* complementation strain. On media plates, *Duba4* radial growth and sporulation rates were significantly ( $P \leq 0.05$ ) reduced compared to WT (**Extended Data Fig. 1a,b**). Reduced radial growth of *M. oryzae* *Duba4* mutant strains is consistent with observations in yeast, where tRNA thiolation is required for optimal nutrient sensing and metabolic homeostasis in a biochemical manner independent of protein translation rates<sup>9</sup>. When equal numbers of *M. oryzae* spores were applied to three-week-old rice seedlings of the susceptible cultivar CO-39, infection with WT and the complementation strain resulted in typical expanded necrotic lesions on leaves by 144 hours post inoculation (hpi), but the *Duba4* mutant strain produced only pinpoint lesions<sup>26</sup> and was thus non-pathogenic (**Fig. 1b**). LC-MS analysis of tRNAs from vegetative mycelia showed that, consistent with

yeast mutants<sup>16</sup>, both the *M. oryzae Duba4* mutant strain and an *Durm1* deletant that we also generated in Guy11, and which was physiologically indistinguishable from *Duba4* (**Extended Data Fig. 1f-k**), were both abolished for the mcm<sup>5</sup>s<sup>2</sup>U tRNA modification (**Fig. 1c**; raw values with replicates in **Extended Data Table 1**), but not for the mcm<sup>5</sup>U tRNA modification (**Extended Data Table 1**), compared to WT. Like in yeast, *M. oryzae Uba4-GFP* localized to the fungal cytoplasm (**Extended Data Fig. 2**). Taken together, we conclude that *M. oryzae UBA4* and *URM1* are required for optimal axenic growth and sporulation, rice plant infection and cytoplasmic tRNA anticodon U<sub>34</sub> thiolation.

After inoculation, *M. oryzae* spores on the host leaf surface germinate and form a specialized dome-shaped infection structure (the appressorium); appressoria adhere to and penetrate the host cuticle under enormous turgor at 24 h post inoculation (hpi)<sup>27,28</sup> and elaborate bulbous, branching invasive hyphae (IH) that fill the first infected rice cell by 44-48 hpi before migrating to neighbouring cells<sup>29</sup>. Live-cell imaging of optically clear detached rice leaf sheaths showed that *UBA4* was not required for leaf cuticle penetration by appressoria (**Extended Data Fig. 1c,d**), or for initial IH elaboration after penetration (**Fig. 1d**), but was essential for filling the first infected rice epidermal cell with IH, and for extensive IH spread to neighbouring cells (**Fig. 1d**; **Extended Data Fig. 1e**). Similar results were obtained for *Durm1* (**Extended Data Fig. 1i-k**). Thus, *UBA4* and *URM1* are required for the *M. oryzae* biotrophic growth phase of living host rice cell invasion.

### Loss of *UBA4* abolishes Pwl2 effector accumulation in the BIC

During biotrophic growth in living rice cells, *M. oryzae* IH are separated from host cytoplasm by an extended interfacial zone comprising host-derived membranes<sup>21,30</sup>. To better understand the role of *UBA4* in biotrophy, we hypothesized that the biotrophic interfacial compartments separating IH from plant host cytoplasm would be perturbed in *Duba4* compared to WT, as observed for other biotrophic growth mutants<sup>30</sup>. WT IH are wrapped in the plant host-derived extra-invasive hyphal membrane<sup>14,29</sup>, forming a matrix into which apoplastic effectors like Bas4 are secreted via the conventional ER-Golgi pathway. A focal, plant-lipid rich membrane structure, the biotrophic interfacial complex (BIC), forms an additional compartment, outside IH, in the first infected rice cell and at the tips of IH spreading to adjacent cells<sup>14,31</sup>. Cytoplasmic effectors like Pwl2 (which confers host species specificity) and AVR-Pita (which confers avirulence on rice lines carrying the corresponding *Pita* R gene) are secreted into the BIC by an unconventional protein secretion pathway before being translocated into the host cell<sup>21</sup>. Effector genes are only expressed *in planta*, therefore fluorescently labelled effectors are cellular probes to monitor both effector deployment and biotrophic interfacial membrane integrity<sup>30</sup>. Using the pBV591 vector<sup>31</sup>, we generated a *Duba4* mutant strain producing, under native promoters, Pwl2 fused to mCherry (which also carries an added C-terminal nuclear localization signal (NLS) to concentrate Pwl2 in the rice nucleus and thus confirm secretion into the host cell<sup>21</sup>), and Bas4 fused to GFP. Using our previously generated *PWL2-mCherry:NLS* and *BAS4-GFP*-expressing strain<sup>32</sup> as a control, we found that at 36 hpi, Bas4-GFP correctly outlined *Duba4* IH (**Fig. 1e**) indicating, contrary to our expectations, that the extra-invasive hyphal membrane was not eroded in *Duba4* and the apoplast was intact. However, whereas

Pwl2-mCherry:NLS accumulated in *UBA4*<sup>+</sup> BICs and was evident in the nuclei of *UBA4*<sup>+</sup>-infected rice cells by 36 hpi (**Fig. 1e**), in contrast, Pwl2-mCherry:NLS was not visible in *Duba4* IH or associated rice nuclei (**Fig. 1e**), suggesting that the *Duba4* BIC was disrupted and/ or unable to receive secreted Pwl2 for translocation into host cells. Together, these initial results suggested that *UBA4*, acting via unspecified means, was required for Pwl2 secretion and accumulation in the BIC, and possibly for BIC integrity, but not for Bas4 secretion or apoplastic space integrity.

### **PWL2 mRNA translation requires the Uba4-Urm1 sulfur relay system**

We initially considered that the loss of Pwl2 secretion and accumulation in *Duba4* BICs indicated BIC integrity (but not apoplast integrity) was disrupted in *Duba4*. However, closer inspection revealed *Duba4* BICs by bright field microscopy and, like for *UBA4*<sup>+</sup> (and as reported by others), Bas4-GFP visibly accumulated under *Duba4* BICs (**Fig. 2a**). Thus, *UBA4* is not required for BIC formation, but is required for Pwl2-mCherry:NLS accumulation in BICs. To understand why Pwl2 did not accumulate in *Duba4* BICs, we considered that in yeast, tRNA anticodon wobble U<sub>34</sub> thiolation by Uba4 prevents ribosome pausing and protein aggregation by improving the efficiency of AA-ending cognate codon decoding<sup>7,17</sup>. We thus hypothesized that the loss of Pwl2 secretion and accumulation in *Duba4* BICs indicated *PWL2-mCherry:NLS* mRNA (but not *BAS4-GFP* mRNA) was translationally impaired *in planta* in the *M. oryzae* *Duba4* mutant strain due to ribosome pausing at AA-ending codons. In yeast, paromomycin treatment mitigates ribosomal pausing at AA-ending codons in U<sub>34</sub> thiolation deficient mutant strains by increasing near-cognate tRNA acceptance<sup>7</sup> (**Fig. 2b**). We infused leaf sheaths with 1 mg ml<sup>-1</sup> paromomycin in 0.2% gelatin at 36 hpi and observed the effects at 44 hpi. In the control *UBA4*<sup>+</sup> strain, *PWL2-mCherry:NLS* mRNA translation and *BAS4-GFP* mRNA translation was not affected by paromomycin treatment as Pwl2-mCherry:NLS and Bas4-GFP were both correctly deployed in IH although, consistent with its role as a protein synthesis inhibitor, *UBA4*<sup>+</sup> IH growth was severely attenuated compared to the untreated control (**Extended Data Fig. 3**). Strikingly, in *Duba4* IH, paromomycin treatment restored Pwl2-mCherry:NLS secretion and accumulation in BICs (**Fig. 2c**). Furthermore, in the *Durm1* mutant strain (which closely resembled *Duba4*, **Extended Data Fig. 1f-k**), we also observed loss of Pwl2-mCherry:NLS accumulation in the *Durm1* BIC, and this was similarly (but weakly) remediated by paromomycin treatment (**Fig. 2d**). Concordant with yeast findings<sup>7</sup>, remediation of Pwl2-mCherry:NLS production by paromomycin suggests that ribosomal pausing is occurring in both the *Duba4* and *Durm1* mutant strains, likely due to inefficient decoding of AA-ending cognate codons. We conclude that the *M. oryzae* Uba4-Urm1 sulfur relay system is required for s<sup>2</sup>U<sub>34</sub> tRNA modification-dependent efficient decoding of *PWL2-mCherry:NLS* mRNA (but not *BAS4-GFP* mRNA) *in planta*.

### **Unconventionally secreted effector protein translation requires wobble U<sub>34</sub> tRNA thiolation**

We next asked if tRNA thiolation was only required for *PWL2* mRNA translation, or whether it was required for other unconventionally secreted cytoplasmic effectors that accumulate in the BIC, of which only few are experimentally determined, including AVR-Pita<sup>31</sup>. To address this, we generated *Duba4* and *UBA4*<sup>+</sup>

strains expressing *BAS4-GFP* along with *AVR-Pita-mCherry:NLS* expressed under its native promoter. **Fig. 3** shows that *AVR-Pita-mCherry:NLS* weakly accumulated in *UBA4*<sup>+</sup> BICs compared to *Pwl2-mCherry:NLS*, as previously described<sup>31</sup>. However, no *AVR-Pita-mCherry:NLS* protein accumulation was observed in *Duba4* BICs unless *Duba4*-infected rice cells were first treated with paromomycin (**Fig. 3**). Therefore, *Uba4*–*Urm1*-dependent wobble  $U_{34}$  tRNA thiolation is required for the translation of unconventionally secreted cytoplasmic effectors during biotrophic growth in host rice cells.

### Synonymous codon recoding remedies *PWL2* mRNA translation in *Duba4*

To confirm that the loss of *PWL2* and *AVR-PITA* (but not *BAS4*) mRNA translation was due to inefficient decoding of AA-ending cognate codons following the loss of tRNA thiolation, we reasoned that recoding AA-ending codons to synonymous AG-ending codons (that are decoded in a  $U_{34}$  modification-independent manner<sup>3,17</sup>) would remediate *PWL2* translation and secretion in the absence of wobble  $U_{34}$  tRNA thiolation. We generated a *Duba4* strain expressing *BAS4-GFP* along with a recoded form of *PWL2-mCherry:NLS* (hereafter termed *PWL2* (-AA<sup>®</sup> -AG)) where all AA-ending codons were recoded to synonymous AG-ending codons (**Fig. 4a** and **Extended Data Fig. 4**). Expressing *PWL2* (-AA<sup>®</sup> -AG) in *Duba4* fully remediated *Pwl2* production and its secretion and accumulation in the *Duba4* BIC (**Fig. 4b**). In some cases, expressing *PWL2* (-AA<sup>®</sup> -AG) resulted in large and/ or unstable *Duba4* BICs (**Extended Data Fig. 5**). Because *PWL2* (-AA<sup>®</sup> -AG) mRNA is under the same promoter and encodes the same amino acid sequence as *PWL2-mCherry:NLS*, we conclude that during host infection, the translation of *PWL2* mRNA (encoding an unconventionally secreted effector) requires wobble  $U_{34}$  tRNA thiolation-dependent efficient decoding of AA-ending cognate codons.

### *PWL2* mRNA abundance is codon-dependent

In addition to *PWL2* mRNA translation, we also found evidence for codon-mediated control of *PWL2* mRNA stability. Quantitative real-time PCR using mCherry-specific primers determined that *PWL2-mCherry:NLS* transcripts were barely detected in *Duba4* IH, but *PWL2* (-AA<sup>®</sup> -AG) mRNA in *Duba4* IH accumulated to levels comparable to *PWL2-mCherry:NLS* mRNA in *UBA4*<sup>+</sup> IH (**Fig. 4c**). These data are suggestive of codon-mediated mRNA decay<sup>33</sup>, potentially No-Go Decay involving endonucleolytic cleavage of mRNAs carrying ribosomes stalled in translation elongation<sup>34,35</sup>. Thus, *PWL2* mRNA abundance in *M. oryzae* IH is dependent on the efficient decoding of AA-ending cognate codons by s<sup>2</sup> $U_{34}$ -modified tRNAs.

### Translation of recoded *BAS4* mRNA with all AA-ending codons does not require $U_{34}$ tRNA thiolation

Why is wobble  $U_{34}$  tRNA thiolation and efficient decoding of AA-ending codons required for *PWL2* and *AVR-PITA* mRNA translation but not for *BAS4* mRNA translation? By comparing AA- and AG-ending codon usage in *BAS4*, *PWL2*, *AVR-PITA* and the *M. oryzae* transcriptome, **Extended Data Fig. 6a** shows that *PWL2* and *AVR-PITA* carry more AA-ending codons than AG-ending codons whereas *BAS4* and the general *M. oryzae* transcriptome predominantly carry AG-ending codons. We thus hypothesized that

codon usage and codon decoding speeds determined effector secretion routes, and we predicted that synonymous AG-ending-to-AA-ending codon changes would abolish *BAS4-GFP* mRNA translation in *Duba4*. To test our hypothesis, we constructed a *Duba4* strain expressing a recoded *BAS4-GFP* gene, *Bas4* (-AG<sup>®</sup> -AA) (**Extended Data Fig. 7**), with no AG-ending codons, along with *PWL2* (-AA<sup>®</sup> -AG) as a control for protein translation. At 36 hpi, this strain accumulated recoded Pwl2 (-AA<sup>®</sup> -AG) in the BIC as expected, but it also correctly deployed recoded Bas4 (-AG<sup>®</sup> -AA) into the apoplast space (**Fig. 4d**; more examples in **Extended Data Fig. 6b**). Thus, contrary to our expectations, at least under the conditions viewed, *UBA4* is not required for the translation of an all AA-ending codon recoded form of *BAS4* mRNA.

Although falsifying our hypothesis, our results are nonetheless consistent with observations in yeast, where the integrity of ER-Golgi proteins was less affected by changes in decoding speeds arising from the loss of U<sub>34</sub> modification than cytosolic proteins, presumably due to different co-translational mechanisms and folding constraints across the ER membrane compared to the cytoplasm<sup>7</sup>. Similarly, our results may suggest unconventionally secreted proteins are folded in different cellular compartments compared to ER-Golgi secreted proteins, with inefficient decoding of AA-ending codons in *Duba4* strains tolerated in the latter but not the former case. Like other *M. oryzae* cytoplasmic effectors, Pwl2 and AVR-Pita<sup>21,31</sup> carry signal peptide sequences targeting them to the ER. Four UPS pathways are known in eukaryotes: Type I-III involve leaderless proteins, but the Type IV pathway secretes proteins with signal peptides that are synthesized on rough ER but bypass the Golgi apparatus<sup>24</sup>. As observed for Pwl2 secretion into the BIC<sup>21</sup>, the Type IV Golgi-bypass pathway is insensitive to Brefeldin A<sup>24</sup>, an inhibitor of ER-to-Golgi transport. Therefore, when considered altogether, our results are consistent with unconventional cytoplasmic effector secretion occurring via a Type IV Golgi-bypass pathway (**Fig. 4e**), which, being intolerant of inefficient AA-ending codon decoding, constitutes a different protein folding environment than the conventional ER-Golgi network.

### **Synonymous recoding of AA-ending codons results in Pwl2 super-secretion in host cells**

Why would *M. oryzae* evolve AA-ending codons in *PWL2* mRNA – whose efficient decoding requires tRNA thiolation by the multi-step Uba4-Urm1 sulfur relay system – when a strain lacking *UBA4* can translate *PWL2* mRNAs carrying all AG-ending synonymous codons instead? To address this question, we expressed *PWL2* (-AA<sup>®</sup> -AG), along with *BAS4-GFP*, in WT. **Fig. 4f** shows that, relative to the *PWL2-mCherry:NLS*-expressing control strain (*Top*), the expression of *PWL2* (-AA<sup>®</sup> -AG) resulted in the formation of giant, brightly fluorescing BICs that were often either unstable and split, or elongated rather than spherical (*Bottom*), suggesting elevated Pwl2 (-AA<sup>®</sup> -AG) translation and secretion into the BIC. Note that Pwl2 (-AA<sup>®</sup> -AG) accumulated in rice nuclei, indicating that the protein was correctly folded and translocated into the host cell. We conclude that AA-ending codon usage in *PWL2* mRNA precisely modulates translation to control Pwl2 production and unconventional secretion into the BIC. In doing so, wobble U<sub>34</sub> tRNA thiolation and codon usage bias directly contribute to BIC integrity during *M. oryzae* biotrophic growth in living rice cells.

## Discussion

To subvert host cell innate immunity, animal and plant microbial pathogens secrete effector proteins and virulence factors<sup>20</sup>, often via unconventional pathways that are much less well understood than conventional ER-Golgi secretion networks<sup>21–24</sup>. Wobble U<sub>34</sub> tRNA thiolation is required for efficient decoding of AA-ending cognate codons to prevent transient ribosome pausing, which affects protein folding<sup>7</sup> and protein homeostasis<sup>17</sup>. However, U<sub>34</sub> thiolation mutants have minor translational defects<sup>9</sup> and specific biological roles for this universal modification are poorly understood. Here, using gene deletions, paromomycin treatment and the synonymous recoding of *PWL2* and *BAS4* mRNA, we connected codon decoding efficiency with protein secretion by determining a specific physiological role for wobble U<sub>34</sub> tRNA thiolation modification and codon usage bias in tuning pathogen unconventional protein secretion in host cells in a manner that maintains microbe-host cell interface stability.

In our study, loss of tRNA thiolation eliminated unconventional protein secretion due to ribosomal pausing, whereas recoded *PWL2* carrying all AG-ending codons resulted in *Pwl2* super-secretion into BICs. Thus, efficient AA-ending codon decoding by wobble s<sup>2</sup>U<sub>34</sub> tRNA anticodons optimizes cytoplasmic effector mRNA translation and unconventional cytoplasmic effector secretion. In *M. oryzae*, BIC-localized cytoplasmic effectors carry signal peptides targeting them to the ER<sup>21</sup>, indicating that unconventional protein secretion occurs via the Golgi-bypass pathway following nascent peptide translocation across the ER<sup>24</sup>. Protein folding constraints in the Golgi-bypass pathway must differ from those of the ER-Golgi pathway because codon recoding or the loss of tRNA thiolation did not affect *BAS4* mRNA translation. Therefore, given that individual codons tightly control local translation elongation rates<sup>19</sup>, evolutionary pressure from effector secretion routes might act at the codon-anticodon interaction level to generate a gene “codon landscape”<sup>36</sup>, whereby intragenic codon frequency bias leads to variable ribosome decoding speeds along an mRNA molecule, thus optimizing co-translational protein folding and protein translocation across membranes<sup>37</sup>. Consequently, unconventionally secreted effector protein genes may evolve tRNA thiolation-dependent codons precisely in order for nascent peptides to be folded correctly within the Golgi-bypass secretion pathway, which is the only means of targeting effector proteins to BICs for entry into host rice cells. Therefore, our results suggest protein folding constraints in the Golgi-bypass pathway shape codon control of protein translation speeds to ensure the integrity of unconventionally secreted effectors.

In addition to tRNA modification, the speed of decoding of a codon by the ribosome also depends on the concentration of the matching tRNA<sup>38</sup>. In general, the most abundant tRNAs pair with the most abundant codons while less abundant tRNAs match less abundant or rare codons<sup>38–40</sup>. tRNA gene copy number is a proxy for relative tRNA isoacceptor abundance<sup>38,39</sup>. According to the tRNAscan-SE analysis of completed genomes, in *M. oryzae*, tRNAs matching the less abundant AA-ending codons are less abundant than tRNAs matching synonymous AG-ending codons for Lys (2 x tK<sup>UUU</sup> genes versus 9 x tK<sup>CUU</sup> genes), Gln (2 x tQ<sup>UUG</sup> genes versus 6 x tQ<sup>CUG</sup> genes) and Glu (3 x tE<sup>UUC</sup> genes versus 9 x tE<sup>CUC</sup> genes).



Thus, compared to *BAS4* mRNA and the general transcriptome, cytoplasmic effector genes are enriched in rare AA-ending codons that are matched to tRNAs in less abundance than those tRNAs that pair with preferred synonymous AG-ending codons. Codons recognizing the same tRNA isoacceptor, including rare codons, are often overrepresented in a gene. This may optimize genes for tRNA reuse, which raises the local concentration of tRNAs, and such genes are expressed more efficiently<sup>38</sup>. Consequently, the use of rare codons in cytoplasmic effector genes that are matched to rare tRNAs may, like U<sub>34</sub> thiolation, also contribute to mRNA translation efficiency and unconventional protein secretion control. Together, these considerations of tRNA gene content suggest that, like in other organisms<sup>38,39</sup>, codon usage bias in *M. oryzae* may be shaped by tRNA abundance, and a detailed investigation of the relationships between tRNA abundance dynamics, tRNA modification and effector secretion is warranted in the future.

By inferring a codon usage code<sup>41</sup> that adapts translation elongation speeds to co-translational protein folding constraints in the Golgi-bypass pathway, our work may help identify new effectors secreted by unconventional routes not only in *M. oryzae*, but also in other plant pathogenic fungi and oomycetes<sup>22</sup>, thereby facilitating the search for novel sources of durable plant host resistance. In addition, parasitic protists including *Leishmania* and the malaria parasite *Plasmodium* traffic virulence factors by unconventional secretion pathways<sup>23</sup>. Our results may aid in deciphering the poorly understood rules of cargo selection, sorting, and translocation<sup>23</sup> in these harrowing agents of human affliction. Together, we have shed new light on a microbial process central to many challenging plant and human diseases.

## Methods

### Fungal strains, culture conditions and physiological analyses

All fungal strains used in this study are listed in **Supplementary Table 1**. The *M. oryzae* isolate Guy11<sup>11</sup> was used as the parental wild type strain. Strains were grown on complete media (CM) plates<sup>28</sup> and were measured and imaged after 10 days growth using a Sony Cyber-shot digital camera (14.1 megapixels). Spores were harvested from 10 days old CM plates and counted in triplicate. Spores for downstream applications were harvested from 12-14 days old oatmeal agar plates (1.5 % w/v prepared using Oatmeal Agar, Bioworld, USA). For whole plant inoculations, spores were applied at a rate of  $1 \times 10^5$  spores ml<sup>-1</sup> to 3-week-old seedlings of the susceptible cultivar CO-39. Infected leaves were harvested, dried and imaged at 5 days post inoculation. Images are representative of at least 5 leaves from each of three independently inoculated plants per strain. Appressorial formation and penetration rates, and cell-to-cell movement rates, were determined by inoculating three detached rice leaf sheaths per strain with  $0.5 \times 10^5$  spores ml<sup>-1</sup>. Leaf sheaths were prepared for microscopy as described previously<sup>28</sup>, and rates were calculated as described in the text.

### Strain construction

*UBA4* and *URM1* were deleted in the Guy11 wild type strain by the PCR-based split-marker method<sup>25</sup> using the primers in **Supplementary Table 2**. Briefly, the coding region of *UBA4* and *URM1* was replaced by the *ILV1* gene conferring sulphonyl urea resistance. At least three independent deletants per gene were confirmed by PCR and subsequently characterized, as detailed in the main text. One deletant of each gene was used to receive the respective add-back complementation vector carrying *UBA4* or *URM1* fused to *GFP*, and to receive vectors carrying *PWL2-mCherry:NLS* and *BAS4-GFP* or codon recoded versions of these genes.

### LC-MS based tRNA modification detection

LC-MS based tRNA modification detection<sup>42,43</sup> was performed by Arraystar Inc., USA, on tRNAs of the indicated strains that were separated from total small RNAs extracted from vegetative hyphae cultured in liquid CM culture for 42 hr. Three biological replicates of each strain were used for the following tRNA modification analysis. After extensive washing with dH<sub>2</sub>O, mycelia were homogenized in liquid nitrogen, and total RNAs were extracted using the TRIzol reagent (Invitrogen, USA), according to the manufacturer's standard procedure. The prepared total RNAs were then subjected to small RNA isolation using the PureLink™ miRNA Isolation Kit (Invitrogen, USA) by following the manufacturer's instruction manual. Small RNA quality was estimated by running on a denatured agarose gel, and the RNA quantity was measured using a Nanodrop Spectrophotometer. More than 10 µg of small RNAs per biological replicate were provided to Arraystar Inc. for further tRNA isolation and modification analysis. There, tRNAs were isolated from small RNAs by 7.5% PAGE (29:1 acrylamide: bisacrylamide) containing 7 M urea. The 60-90 nt band of tRNA was excised from the gel, extracted with 0.3 M NH<sub>4</sub>Ac and precipitated with glycogen and ethanol, then quantified using the Qubit RNA HS Assay kit (ThermoFisher, USA). Purified tRNA was hydrolyzed to single, dephosphorylated nucleosides in a 50 µL reaction volume containing 10 U Benzonase (Sigma, USA), 0.1 U Phosphodiesterase I (US Biological, USA) and 1U Alkaline Phosphatase (NEB, USA) following incubation at 37 °C for 3 hr. The hydrolyzed nucleoside solution was deproteinized using a Satorius 10,000-Da MWCO spin filter. The mononucleoside analytes were then separated on an Agilent Zobax SB-Aq liquid chromatography column with flow rate determined by a solvent gradient generated from mixing Solution A (0.1% (vol/vol) final concentration of formic acid in HPLC-grade water) and Solution B (0.1% (vol/vol) final concentration of formic acid in 100% acetonitrile). tRNA modifications including mcm<sup>5</sup>s<sup>2</sup>U and mcm<sup>5</sup>U were identified by an Agilent 6460 Triple Quadrupole mass analyzer running in MRM mode at the parent to daughter ion transition of (m/z 333.0→201.0). LC-MS data was acquired using Agilent Qualitative Analysis software. MRM peaks of each modified nucleoside were extracted and normalized to the quantity of purified tRNA for each sample.

### Live-cell imaging

For live-cell imaging of fluorescent fusion proteins, 3- to 4-week-old rice leaf sheaths of the susceptible cultivar CO-39 were inoculated with 1×10<sup>5</sup> spores ml<sup>-1</sup> of the indicated strains. For each strain, time points and treatments were repeated at least three independent times. 1 mg ml<sup>-1</sup> paromomycin (Sigma-Aldrich, USA) in 0.2% gelatin was added to cells at 36 hpi and its effects observed at 44 hpi. Infected

detached rice leaf sheaths were imaged using a Nikon Eclipse Ni-E upright microscope and NIS Elements software. Excitation/emission was 488 nm/505–531 nm for GFP and 543 nm/590–632 nm for mCherry.

## Vector construction

The primers used for constructing the *UBA4-GFP* and *URM1-GFP* complementation vectors are in **Supplementary Table 2**. Briefly, *UBA4* and *URM1* were amplified with the indicated primers to produce PCR products with 15~20 bases homologous to the pGTN vector. Purified PCR product was fused with linearized pGTN using the In-Fusion HD Cloning Kit (Clontech, USA). The ligation was transferred into the *E. coli* DH5a strain with ampicillin antibiotic screening, and all colonies were identified by PCR. Plasmids were sequenced to confirm they were error-free, then transformed into *M. oryzae* strains. *M. oryzae* transformants were screened by geneticin resistance and confirmed by PCR.

Recoded plasmids were constructed at GenScript USA, Inc., using the vector pBV591 as template, whereby the *PWL2* (-AA<sup>®</sup> -AG) sequence replaced *PWL2-mCherry:NLS. BAS4-GFP* in this *PWL2* (-AA<sup>®</sup> -AG)-carrying vector was then replaced with *Bas4* (-AG<sup>®</sup> -AA). Similarly, the *PWL2* sequence and native promoter were replaced in pBV591 by *AVR-PITA* and its native promoter to generate *AVR-PITA-mCherry:NLS* (along with *BAS4-GFP*). The *PWL2* (-AA<sup>®</sup> -AG), *Bas4* (-AG<sup>®</sup> -AA) and *AVR-PITA* genes were synthesized at GenScript USA, Inc., cloned onto their respective vectors using the Clone EZ cloning method and confirmed by sequencing.

## Quantitative real-time PCR

Leaf sheath samples were harvested at 42 hpi and total RNA was extracted from each sample using the RNeasy mini kit (Qiagen, USA). RNA was treated with DNase I (Invitrogen, USA) and converted to cDNA using qScript (Quantas, USA). qPCR was performed on an Eppendorf Mastercycler Realplex using the recommended reagents with primers listed in **Supplementary Table 2**. Thermocycler conditions were: 5 min at 95 °C, followed by 40 cycles of 95 °C for 30 sec, 63 °C for 30 sec and 68 °C for 1 min. qPCR data was analyzed using the Realplex software package and fold changes were calculated using the  $\Delta\Delta C_t$  method<sup>44</sup>.

## Codon usage and tRNA abundance analysis

The complete CDS database of *Magnaporthe oryzae*, which contains 12836 cDNAs, was obtained from the JGI Genome portal ([https://genome.jgi.doe.gov/portal/pages/dynamicOrganismDownload.jsf?organism=Magor1, Project name: \*Pyricularia oryzae\* 70-15 v3.0](https://genome.jgi.doe.gov/portal/pages/dynamicOrganismDownload.jsf?organism=Magor1,Project%20name%3A%20Pyricularia%20oryzae%2070-15%20v3.0)). The codon usage pattern was analyzed with the CUSP program of EMBOSS (The European Molecular Biology Open Software Suite, Cambridge, UK; <http://bioinfo.pbi.nrc.ca:8090/EMBOSS/>) utilizing the high performance computing resources provided by the Holland Computing Center at the University of Nebraska-Lincoln. tRNA gene abundance estimates were obtained from the tRNAscan-SE analysis of the *M. oryzae* genome deposited at the Genomic tRNA Database ([http://lowelab.ucsc.edu/GtRNAdb/Magn\\_oryz\\_70-15/Magn\\_oryz\\_70-15-summary.html](http://lowelab.ucsc.edu/GtRNAdb/Magn_oryz_70-15/Magn_oryz_70-15-summary.html)).

## Statistical analysis

For comparing the mean values of the colony diameters, sporulation rates, appressorium formation rates, penetration rates and cell-to-cell movement rates, the one-way ANOVA function in PASW Statistics 18.0 (PASW Statistics Inc.) with a Student-Newman-Keuls multiple comparison test was used. For comparing target gene expression levels between different strains, the quantified transcript abundance was calculated as the fold change as described in the figure legends and statistical analysis was carried out using one-way ANOVA with the Student-Newman-Keuls multiple comparison tests in PASW Statistics. A resulting *P* value of less than 0.05 was considered significant between group means.

## Reporting Summary

Further information on research design is available in the Nature Research Reporting Summary linked to this article.

## Data availability

The *M. oryzae* *UBA4* and *URM1* gene sequences are available at NCBI under the accessions MGG\_05569 and MGG\_03978, respectively. Data supporting the findings of this study are available from the corresponding author upon request. Strains generated during the course of this study are available from the corresponding author upon request and with an appropriate APHIS permit.

## References

1. Björk, G. R., Huang, B., Persson, O. P. & Byström, A. S. A conserved modified wobble nucleoside (mcm<sup>5</sup>s<sup>2</sup>U) in lysyl-tRNA is required for viability in yeast. *RNA* **13**,1245–1255 (2007).
2. Dewez, M. et al. The conserved Wobble uridine tRNA thiolase Ctu1-Ctu2 is required to maintain genome integrity. *Proc. Natl. Acad. Sci. U.S.A.* **105**, 5459–5464 (2008).
3. Rezgui, V. A. et al. tRNA t<sup>KUUU</sup>, tQ<sup>UUG</sup>, and tE<sup>UUC</sup> wobble position modifications fine-tune protein translation by promoting ribosome A-site binding. *Proc. Natl. Acad. Sci. U. S. A.* **110**,12289–12294 (2013).
4. Zinshteyn, B. & Gilbert, W. V. Loss of a conserved tRNA anticodon modification perturbs cellular signaling. *PLoS Genet.* **9**, e1003675 (2013).
5. Boccaletto, P. et al. MODOMICS: a database of RNA modification pathways. *Nucleic Acids Res.* **46**, D303-D307 (2018).
6. Laxman, S. et al. Sulfur amino acids regulate translational capacity and metabolic homeostasis through modulation of tRNA thiolation. *Cell* **154**, 416–429 (2013).
7. Nedialkova, D. D. & Leidel, S. A. Optimization of Codon Translation Rates via tRNA Modifications Maintains Proteome Integrity. *Cell* **161**, 1606–1618 (2015).

8. Chou, H. J. et al. Transcriptome-wide Analysis of Roles for tRNA Modifications in Translational Regulation. *Mol. Cell* **68**, 978–992 (2017).
9. Gupta, R. et al. A tRNA modification balances carbon and nitrogen metabolism by regulating phosphate homeostasis. *Elife* **8**, e44795 (2019).
10. Dean, R. A. et al. The genome sequence of the rice blast fungus *Magnaporthe grisea*. *Nature* **434**, 980–986 (2005).
11. Wilson, R. A. & Talbot, N. J. Under pressure: investigating the biology of plant infection by *Magnaporthe oryzae*. *Nat. Rev. Microbiol.* **7**, 185–95 (2009).
12. Fernandez, J. & Orth, K. Rise of a Cereal Killer: The Biology of *Magnaporthe oryzae* Biotrophic Growth. *Trends Microbiol.* **26**, 582–597 (2018).
13. Cruz-Mireles, N., Eseola, A. B., Osés-Ruiz, M., Ryder, L. S. & Talbot, N. J. From appressorium to transpressorium-Defining the morphogenetic basis of host cell invasion by the rice blast fungus. *PLoS Pathog.* **17**, e1009779 (2021).
14. Wilson, R. A. *Magnaporthe oryzae*. *Trends Microbiol.* **29**, 663–664 (2021).
15. Pabis, M. et al. Molecular basis for the bifunctional Uba4-Urm1 sulfur-relay system in tRNA thiolation and ubiquitin-like conjugation. *EMBO J.* **39**, e105087 (2020).
16. Leidel, S. et al. Ubiquitin-related modifier Urm1 acts as a sulphur carrier in thiolation of eukaryotic transfer RNA. *Nature* **458**, 228–232 (2009).
17. Rapino, F. et al. Wobble tRNA modification and hydrophilic amino acid patterns dictate protein fate. *Nat. Commun.* **12**, 2170 (2021).
18. Shigi, N. Recent Advances in Our Understanding of the Biosynthesis of Sulfur Modifications in tRNAs. *Front. Microbiol.* **9**, 2679 (2018).
19. Rapino, F. et al. Codon-specific translation reprogramming promotes resistance to targeted therapy. *Nature* **558**, 605–609 (2018).
20. Stuart, L. M., Paquette, N. & Boyer, L. Effector-triggered versus pattern-triggered immunity: how animals sense pathogens. *Nat. Rev. Immunol.* **13**, 199–206 (2013).
21. Giraldo, M. C. et al. Two distinct secretion systems facilitate tissue invasion by the rice blast fungus *Magnaporthe oryzae*. *Nat. Commun.* **4**, 1996 (2013).
22. Liu, T. et al. Unconventionally secreted effectors of two filamentous pathogens target plant salicylate biosynthesis. *Nat. Commun.* **5**, 4686 (2014).
23. Balmer, E. A. & Faso, C. The Road Less Traveled? Unconventional Protein Secretion at Parasite-Host Interfaces. *Front. Cell Dev. Biol.* **9**, 662711 (2021).
24. Rabouille, C. Pathways of Unconventional Protein Secretion. *Trends Cell Biol.* **27**, 230–240 (2017).
25. Wilson, R. A., Gibson, R. P., Quispe, C. F., Littlechild, J. A., Talbot, N. J. An NADPH-dependent genetic switch regulates plant infection by the rice blast fungus. *Proc. Natl. Acad. Sci. U. S. A.* **107**, 21902–21907 (2010).

26. Valent, B., Farrall, L. & Chumley, F. G. *Magnaporthe grisea* genes for pathogenicity and virulence identified through a series of backcrosses. *Genetics* **127**, 87–101 (1991).
27. Ryder, L. S. et al. A sensor kinase controls turgor-driven plant infection by the rice blast fungus. *Nature* **574**, 423–427 (2019).
28. Rocha, R. O., Elowsky, C., Pham, N. T. T. & Wilson, R. A. Spermine-mediated tight sealing of the *Magnaporthe oryzae* appressorial pore-rice leaf surface interface. *Nat. Microbiol.* **5**, 1472–1480 (2020).
29. Kankanala, P., Czymmek, K. & Valent, B. Roles for rice membrane dynamics and plasmodesmata during biotrophic invasion by the blast fungus. *Plant Cell* **19**, 706–724 (2007).
30. Sun, G., Elowsky, C., Li, G. & Wilson RA. TOR-autophagy branch signaling via Imp1 dictates plant-microbe biotrophic interface longevity. *PLoS Genet.* **14**, e1007814 (2018).
31. Khang, C. H. et al. Translocation of *Magnaporthe oryzae* effectors into rice cells and their subsequent cell-to-cell movement. *Plant Cell* **22**, 1388–1403 (2010).
32. Marroquin-Guzman, M. et al. The *Magnaporthe oryzae* nitrooxidative stress response suppresses rice innate immunity during blast disease. *Nat. Microbiol.* **2**, 17054 (2017).
33. Mishima, Y., Han, P., Ishibashi, K., Kimura, S. & Iwasaki, S. Ribosome slowdown triggers codon-mediated mRNA decay independently of ribosome quality control. *EMBO J.* **4**, e109256 (2022).
34. Doma, M. K. & Parker, R. Endonucleolytic cleavage of eukaryotic mRNAs with stalls in translation elongation. *Nature* **440**, 561–564 (2006).
35. Navickas, A. et al. No-Go Decay mRNA cleavage in the ribosome exit tunnel produces 5'-OH ends phosphorylated by Trl1. *Nat. Commun.* **11**, 122 (2020).
36. Quax, T. E., Claassens, N. J., Söll, D. & van der Oost, J. Codon Bias as a Means to Fine-Tune Gene Expression. *Mol. Cell* **59**, 149–61 (2015).
37. Pechmann, S., Chartron, J. W. & Frydman, J. Local slowdown of translation by nonoptimal codons promotes nascent-chain recognition by SRP in vivo. *Nat. Struct. Mol. Biol.* **21**, 1100–1105 (2014).
38. Novoa, E. M. & Ribas de Pouplana, L. Speeding with control: codon usage, tRNAs, and ribosomes. *Trends Genet.* **28**, 574–581 (2012).
39. Novoa, E. M., Pavon-Eternod, M., Pan, T. & Ribas de Pouplana, L. A role for tRNA modifications in genome structure and codon usage. *Cell* **149**, 202–213 (2012).
40. Qian, W., Yang, J. R., Pearson, N. M., Maclean, C. & Zhang, J. Balanced codon usage optimizes eukaryotic translational efficiency. *PLoS Genet.* **8**, e1002603 (2012).
41. Liu, Y. A code within the genetic code: codon usage regulates co-translational protein folding. *Cell Commun. Signal.* **18**, 145 (2020).
42. Yan, M. et al. A high-throughput quantitative approach reveals more small RNA modifications in mouse liver and their correlation with diabetes. *Anal. Chem.* **85**, 12173–12181 (2013).
43. Su, D. et al. Quantitative analysis of ribonucleoside modifications in tRNA by HPLC-coupled mass spectrometry. *Nat. Protoc.* **9**, 828–41 (2014).

44. Livak, K. J. & Schmittgen, T. D. Analysis of Relative Gene Expression Data Using Real-Time Quantitative PCR and the  $2^{-\Delta\Delta CT}$  Method. *Methods* **25**, 402–408 (2001).

## Declarations

### Acknowledgements

This work was supported by the National Science Foundation (IOS-1758805). Z.G. was supported by funding from the China Scholarship Council (file no. 201903250119). Bioinformatic analyses were completed using the supercomputing resources of the Holland Computing Center at the University of Nebraska-Lincoln, which receives support from the Nebraska Research Initiative.

### Author contributions

R.A.W. conceived the project and obtained funding. R.A.W. designed the experiments; R.A.W. and G.L. interpreted the data. G.L., Z.G. and N.D. generated the strains and performed the experiments. G.L. performed the bioinformatic analyses. R.A.W. wrote the manuscript, with contributions from all authors.

### Competing interests

The authors declare no competing interests.

### Additional information

**Extended data** is available for this paper.

**Supplementary information** is available for this paper.

**Correspondence and requests for materials** should be addressed to Richard A. Wilson.

## Figures

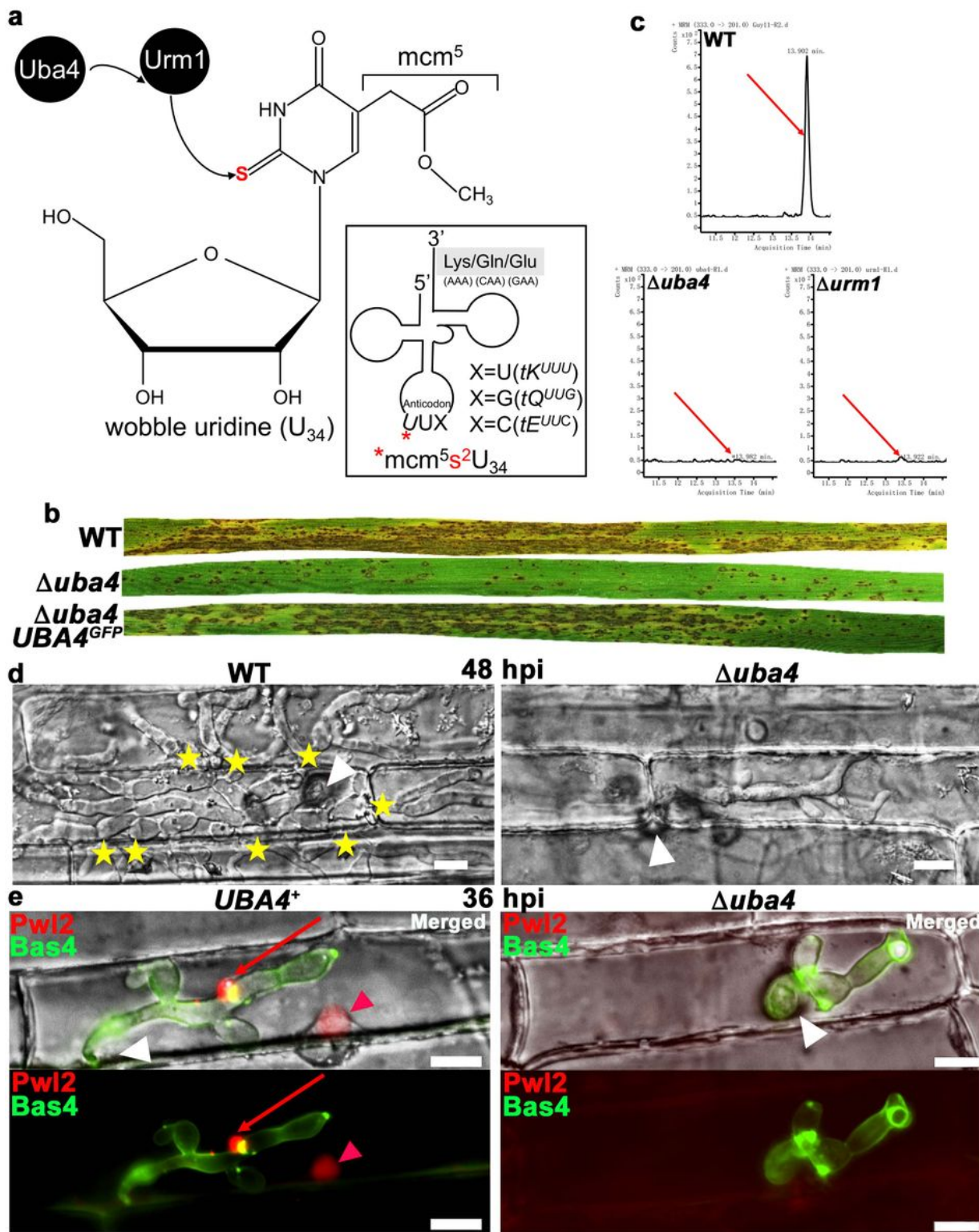


Figure 1

**Wobble uridine tRNA thiolation is required for fungal pathogenicity.** **a**, Thiolation of wobble  $U_{34}$  at tRNA anticodons corresponding to AA-ending codons is by the widely conserved Uba4-Urm1 sulfur relay system<sup>7</sup>. **b**, The *M. oryzae* *UBA4* gene is required for pathogenicity on leaves of the susceptible rice cultivar CO-39. Spores of the indicated strains were sprayed on three-week-old seedlings at a rate of  $1 \times 10^5$  spores  $ml^{-1}$ . Images were taken at 5 days post infection. **c**, Mass chromatograms of the  $mcm^5s^2U$



tRNA modification in vegetative mycelia of the indicated strains. Y axes are ion counts, X axes are acquisition time. The expected  $mcm^5s^2U$  modification peak positions are indicated by arrows. **d**, Live-cell imaging at 44 hours post inoculation (dpi) of detached rice leaf sheath epidermal cells colonized with the indicated strains. White arrowheads indicate penetration sites, stars indicate movement of invasive hyphae into neighbouring cells. Bar is 10  $\mu$ m. **e**, Live-cell imaging at 36 hpi of detached rice leaf sheath epidermal cells colonized with the indicated strains carrying genes encoding the cytoplasmic effector Pwl2-mCherry:NLS and the apoplastic effector Bas4-GFP. White arrowheads indicate penetration sites, red arrowheads indicate Pwl2 in host nuclei, red arrows indicate Pwl2 in BICs. Bar is 10  $\mu$ m.

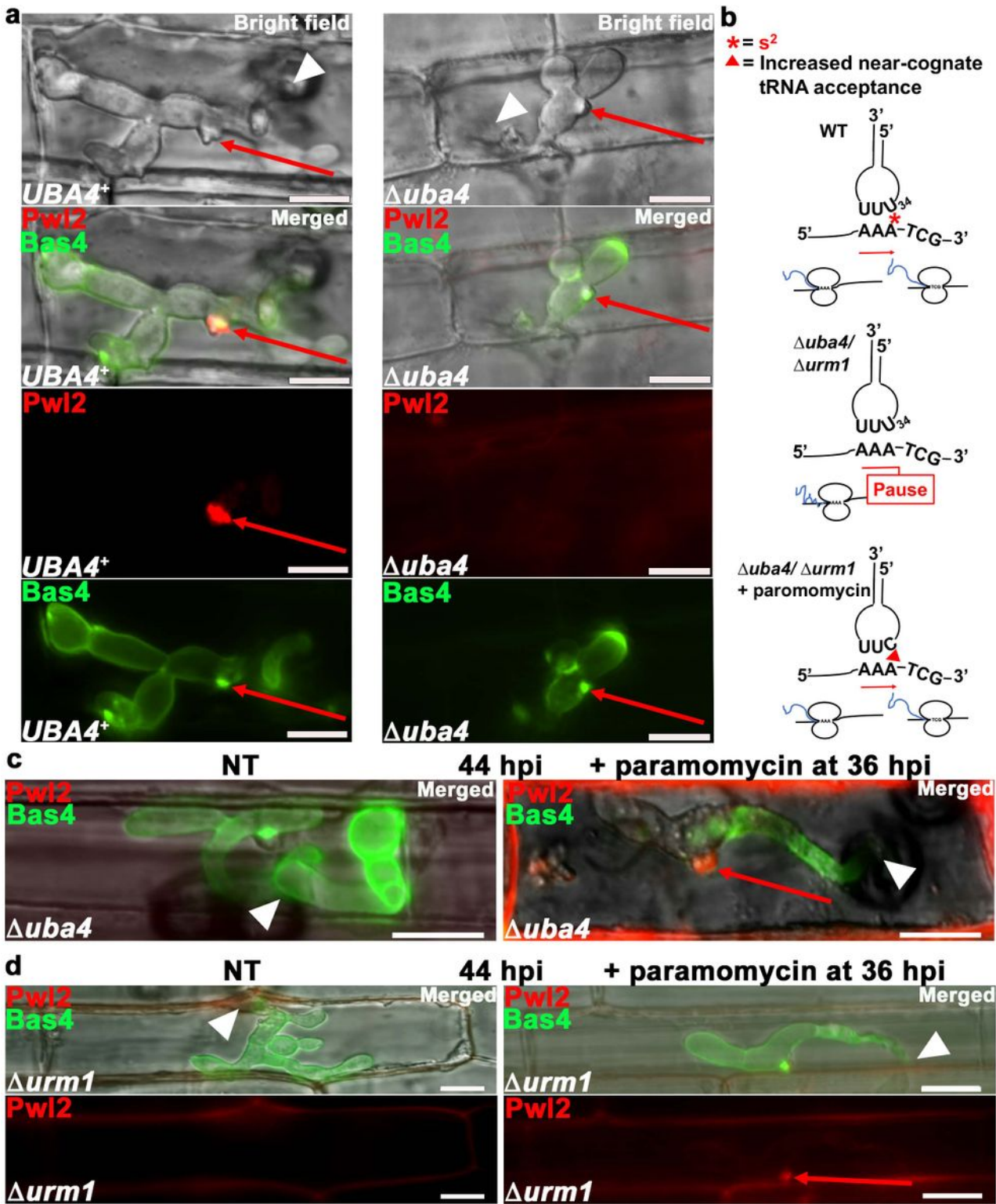


Figure 2

tRNA thiolation is required for *PWL2* mRNA translation. **a**, The *Duba4* strain does not accumulate Pwl2 in BICs. Live-cell images of detached rice leaf sheath epidermal cells were taken at 36 hpi. White arrowheads indicate penetration sites, red arrows indicate BICs. Bar is 10 μm. **b**, Example illustrating how paromomycin treatment<sup>7</sup> increases near-cognate tRNA acceptance to prevent ribosome pausing in *Duba4* and *Durm1* strains. **c,d**, Paromomycin treatment of detached rice leaf sheath epidermal cells colonized

with the indicated mutant strains at 36 hpi restored Pwl2 translation by 44 hpi. White arrowheads indicate penetration sites, red arrows indicate Pwl2 in BICs. Bar is 10 mm. NT is no treatment.

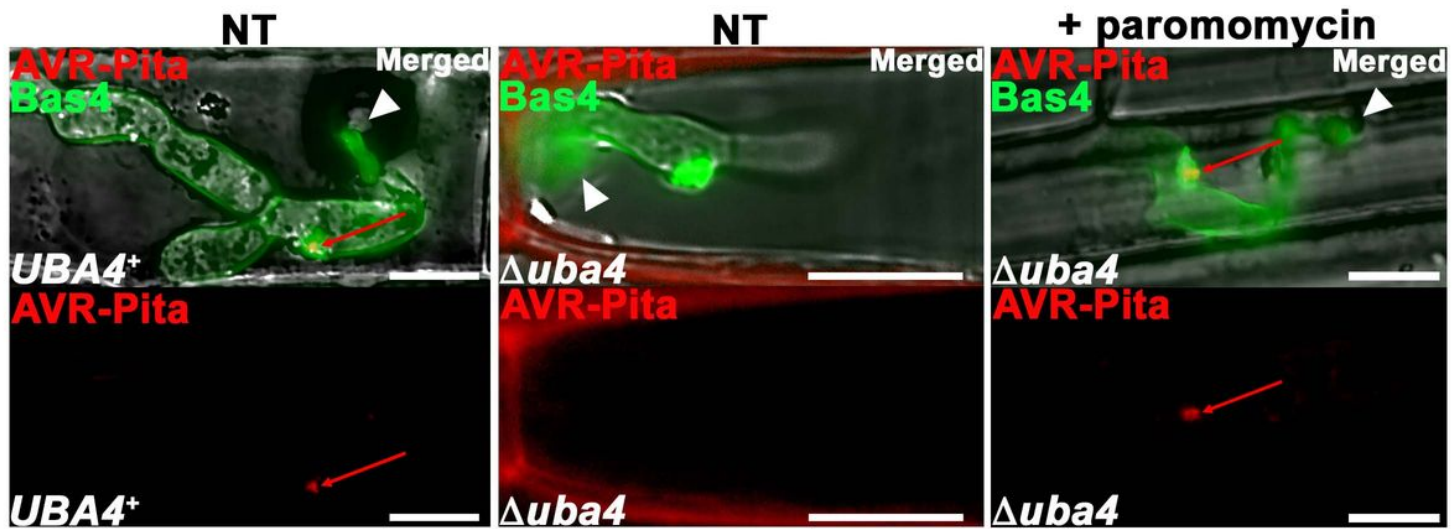


Figure 3

**Translation of unconventionally secreted effectors but not ER-Golgi secreted effectors requires tRNA thiolation.** Live cell-imaging at 44 hpi of detached rice leaf sheath epidermal cells shows that in *UBA4*<sup>+</sup>, AVR-Pita is secreted into the BIC, but the accumulation of AVR-Pita in BICs is abolished in the *Duba4* strain unless first treated with paromomycin at 36 hpi. White arrowheads indicate penetration sites, red arrows indicate AVR-Pita in BICs. Bar is 10 mm. NT is no treatment.

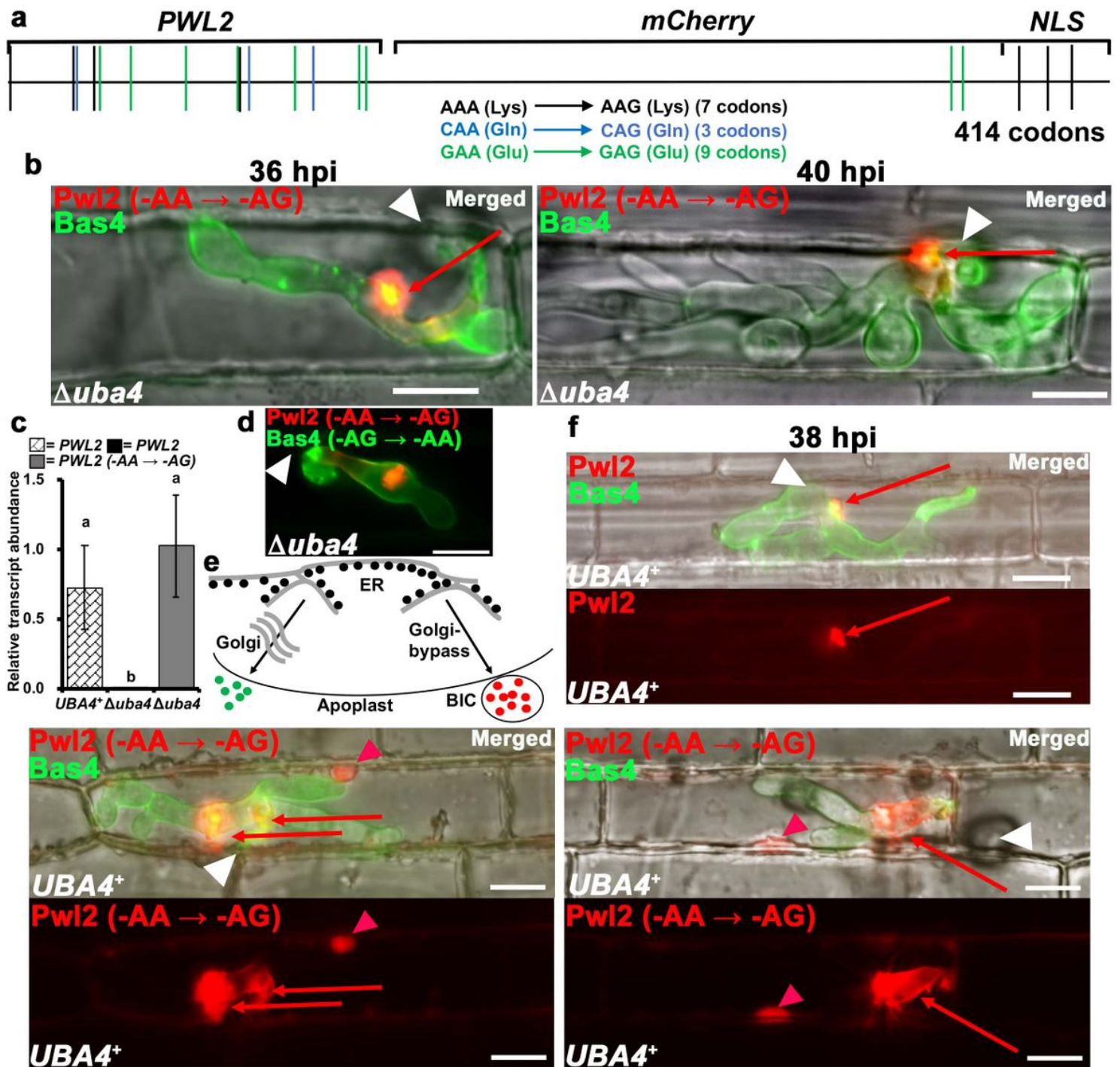


Figure 4

tRNA thiolation and codon usage tune unconventional protein secretion in host cells. **a**, Synonymous codon changes in *PWL2-mCherry:NLS* to yield *PWL2* (-AA<sup>®</sup> -AG). **b**, Live-cell imaging at 36 hpi and 40 hpi of detached rice leaf sheath epidermal cells infected with *Duba4* shows *PWL2* mRNA translation is remediated by synonymous codon recoding. **c**, Using *mCherry*-specific primers, quantitative real-time PCR analysis of cDNAs obtained at 42 hpi from detached rice leaf sheaths infected with the indicated strains shows that *PWL2* mRNA abundance is codon-dependent. Values are the mean of three independent replicates and were calculated for each strain by normalizing the expression of *PWL2-mCherry:NLS* or

*PWL2* (-AA<sup>®</sup> -AG) against the *M. oryzae* actin-encoding gene *MoACT*, then normalizing these values against the relative transcript abundance of *PWL2-mCherry:NLS* in *UBA4<sup>+</sup>*. Error bars are sd. Bars with the same letter are not significantly different (Student-Newman-Keuls test,  $P \leq 0.05$ ). **d**, Synonymous AG-ending to AA-ending codon changes in *BAS4-GFP* did not affect Bas4-GFP secretion in *Duba4*. Images were taken at 36 hpi. White arrowheads indicate penetration sites. Bar is 10 mm. **e**, Unconventionally secreted effectors requiring wobble U<sub>34</sub> tRNA thiolation carry signal peptides and are likely secreted through the Golgi-bypass pathway<sup>24</sup>, where they may be subjected to different folding constraints during translation compared to conventional ER-Golgi secreted proteins, which do not require U<sub>34</sub> tRNA thiolation. **f**, Live-cell imaging at 38 hpi of detached rice leaf sheaths infected with the indicated strains shows that compared to the *PWL2-mCherry:NLS*-expressing *UBA4<sup>+</sup>* control strain (*Top*), expressing *PWL2* (-AA<sup>®</sup> -AG) in *UBA4<sup>+</sup>* results in recoded Pwl2 super-secretion into BICs, which are destabilized (*Bottom*). **b**, **f**, White arrowheads indicate penetration sites, red arrowheads indicate recoded Pwl2 in host nuclei, red arrows indicate Pwl2 (**b**) and recoded Pwl2 (**f**) in BICs. Bar is 10 mm.

## Supplementary Files

This is a list of supplementary files associated with this preprint. Click to download.

- [SupplementaryTable1.docx](#)
- [SupplementaryTable2.docx](#)
- [ExtendedDataTable1.xlsx](#)
- [ExtendedData.docx](#)